Authors Queries

Journal: **International Journal of Remote Sensing**
Paper: **224952**
Title: **The use of high-resolution image time series for crop classification and evapotranspiration estimate over an irrigated area in central Morocco**

224952

Dear Author
During the preparation of your manuscript for publication, the questions listed below have arisen. Please attend to these matters and return this form with your proof. Many thanks for your assistance

Query Reference	Query	Remarks
1	FAO – Please expand index names at first occurrence.	
2	ALADIN – Please expand index names at first occurrence.	
3	Maisongrande 1995 changed to Maisongrande et al. 1995 in text to match reference list. Okay?	
4	Moulin 1997 changed to Moulin et al. 1997 in text to match reference list. Okay?	
5	Duchemin 1999 changed to Duchemin et al. 1999 in text to match reference list. Okay?	
6	Gutmann 1999 in text but Gutman 1999 in reference list. Please check/correct spelling.	
7	Bastiaanssen 2000a changed to Bastiaanssen et al. 2000 in text to match reference list. Okay?	
8	Hunsaker 2003 changed to Hunsaker et al. 2003 in text to match reference list. Okay?	
9	FAO – Please expand index names at first occurrence.	

International Journal of Remote Sensing **res112815.3d** 6/3/07 17:18:08
The Charlesworth Group, Wakefield +44(0)1924 369598 - Rev 7.51n/W (Jan 20 2003)

10	Allen 1998 changed to Allen et al. 1998 in text to match reference list. Okay?	
11	SEBAL – Please expand index names at first occurrence.	
12	Calera et al. 2003 changed to Calera Belmonte et al. 2003 in text to match reference list. Okay?	
13	ALADIN – Please expand index names at first occurrence.	
14	ARPEGE – Please expand index names at first occurrence.	
15	SMAC – Please expand index names at first occurrence.	
16	Duchemin 2006 changed to Duchemin et al. 2006 in text to match reference list. Okay?	
17	LAI – Please provide LAI in full at first occurrence.	
18	Commission error in table heading changed to Omission error. Correct?	
19	FAO – Please expand index names at first occurrence.	
20	SPOT, IRS, FORMOSAT – Please expand index names at first occurrence.	
21	SMOS – Please expand index names at first occurrence.	
22	Calera Belmonte et al. 2003 – Please provide further publication details including editor(s), publisher and publisher location and page range or URL and access date.	

International Journal of Remote Sensing **res112815.3d** 6/3/07 17:18:18
The Charlesworth Group, Wakefield +44(0)1924 369598 - Rev 7.51n/W (Jan 20 2003)

International Journal of Remote Sensing res112815.3d 6/3/07 17:18:18
The Charlesworth Group, Wakefield +44(0)1924 369598 - Rev 7.51n/W (Jan 20 2003)

23	Carlotto 1998 – Not found in text. Please cite or remove from reference list.	
24	Chehbouni et al. 2003 – Please provide further publication details including editor(s), publisher and publisher location and page range or URL and access date.	
25	Chern et al. 2001 – Please provide further publication details including editor(s), publisher and publisher location and page range or URL and access date.	
26	Dedieu et al. 2003 – Please provide further publication details including editor(s), publisher and publisher location and page range or URL and access date.	
27	De Fries et al. 1998 – Not found in text. Please cite or remove from reference list.	
28	Er-Raki et al. 2006 – Publication update available? Please update.	
29	Gutmann 1999 in text but Gutman 1999 in reference list. Please check/correct spelling.	
30	Hadria et al. 2006a – Publication update available? Please update.	
31	Hadria et al. 2006b – Publication update available? Please update.	
32	Simonneaux et al. 2001 – Please provide further publication details including editor(s), publisher and publisher location and page range or URL and access date.	

International Journal of Remote Sensing
Vol. 000, No. 000, 0 Month 2007, 1–22

Taylor & Francis
Taylor & Francis Group

The use of high-resolution image time series for crop classification and evapotranspiration estimate over an irrigated area in central Morocco

V. SIMONNEAUX*†, B. DUCHEMIN†, D. HELSON†, S. ER-RAKI‡, A. OLIOSO§ and A. G. CHEHBOUN†

†CESBIO (Centre d'Etudes Spatiales de la Biosphère), 18 Avenue Edouard Belin, BPI 2801, 31401 Toulouse Cedex 9, France
‡Faculté des Sciences Semlalia, Marrakech, Marocco
§Institut National de Recherche Agronomique, Avignon, France

(*Received 4 May 2006; in final form 19 December 2006*)

A time series of ten high-resolution Landsat TM images, ranging over the crop season, has been acquired over an irrigated area in central Morocco. From this time series, a Normalized Difference Vegetation Index (NDVI) profile was generated for each pixel. In order to get significant profiles, the images were radiometrically corrected, first, using invariant objects located on the scene, based on visual observation of the images, and second, using the reflectance of these objects, estimated from a previously corrected image. In the following step, these NDVI profiles were used to identify four main crop types—bare soil, annual crops, trees on bare soil and trees on annual understory—using a decision tree algorithm. The resulting land cover map and the associated NDVI profiles were then used for an evapotranspiration estimate over the whole area, using the FAO model. Daily outputs of the Moroccan meteorological model ALADIN were used to generate reference evapotranspiration (ET_0) maps and K_c estimates were determined using the NDVI profiles.

1. Introduction

Water management is a major issue in arid lands, especially those having large irrigated areas. Optimization of irrigation water—using only what is actually needed by plants—is one of the obvious ways to save water. In order to monitor plant water requirements over large areas, remote sensing is a very interesting tool that gives synoptic information about two key parameters for evapotranspiration (ET) assessment: land cover and crop development. Remote sensing capabilities for monitoring vegetation and its physical properties have been identified for years now (Tucker 1979). The interest of image time series for vegetation monitoring has also been pointed out, mainly with regard to low-resolution images, which have been available for a long time (Maisongrande *et al.* 1995, Moulin *et al.* 1997, Duchemin *et al.* 1999, Gutmann 1999). Remote sensing potential for monitoring irrigated crops using high-resolution images was more recently discussed (Allen 2000, Bastiaanssen *et al.* 2000, Hunsaker *et al.* 2003). Regarding irrigation, two main approaches may be considered: the first, using optical information to estimate vegetation development through the computation of vegetation indexes—for example, as in the FAO model (Allen *et al.* 1998); the second, using both optical and thermal bands

*Corresponding author. Email: simonneaux@ird.fr

International Journal of Remote Sensing
ISSN 0143-1161 print/ISSN 1366-5901 online © 2007 Taylor & Francis
http://www.tandf.co.uk/journals
DOI: 10.1080/01431160701250390

to assess instantaneous energy balance of vegetation and thus its possible stress, as in the SEBAL model (Baastianssen 2000). We focus here more specifically on the potential of high-resolution optical image time series for irrigated vegetation monitoring. The usefulness of such time series for operational agronomic applications is currently a subject of investigation (Calera Belmonte *et al.* 2003), as this type of data is becoming more easily available through new missions like ROCSAT/FORMOSAT (Chern *et al.* 2001), or planned ones like RHEA (Dedieu *et al.* 2003). The inherent pointing capabilities of these new sensors are similar to those of SPOT HRV, which enables revisiting, thus making them much more efficient than Landsat TM for time series acquisition.

The study area is located in the irrigated Haouz plain, around Marrakech, Morocco. Irrigation management in this area would benefit from better estimates of actual water consumption, as water is being distributed on a fixed, per-area basis. A time series of eight Landsat TM images was acquired over the six-month growing season, from November 2002 to May 2003. This paper presents the full process used for analysing this time series for ET estimate of the vegetation over the area, including the three steps of (i) radiometric correction, (ii) land cover characterization, and (iii) phenology monitoring. We show here how such image time series, apart from allowing an accurate monitoring of the crop cycle, may be useful to simply identify crops, where ordinary classification methods may fail because of the very important variations of phenology within each crop class.

2. Material and methods

2.1 *Study area*

The Haouz plain, around Marrakech, is located in central Morocco, to the north of the High Atlas mountain range (figure 1). The climate of the area is markedly contrasted over the course of the year: hot and dry in the summer, with almost no rainfall except for some violent storms in the mountains; from autumn to spring, the temperature decreases and there is rainfall. Precipitation varies from 240 mm a^{-1} in the Haouz plain to about 500 mm a^{-1} in the mountains located south of the plain, with great inter- and intra-annual variability. Water descending from the mountains is stored in some large dams and is mainly used for irrigation of the Haouz plain. This water is distributed throughout the year, but especially during the rainy season—from late autumn to spring—to complement insufficient rainfall. The irrigated area covers approximately 3000 km^2. The main crops are tree plantations (olive, citrus trees and apricot), covering about 38% of the irrigated areas, and very often combined with understory composed of various annuals, mainly wheat or grass, which is used as forage. The approximately 60% of the remaining irrigated area is used for herbaceous crop production (mainly annuals, like wheat and barley, with some alfalfa). The actual annual crop area is subject to high variations depending mainly on the water available in the dams at the beginning of the crop season, as well as the rainfall occurring during autumn, which affects the sowings date of the farmers. The period of maximum annual crop density therefore occurs during the winter, while in summer only perennial tree crops remain.

2.2 *Data*

The eight TM scenes acquired, which range over the six months of vegetation development, are dated as follows: 7 November 2002, 25 December 2002, 26

224952
International Journal of Remote Sensing res112815.3d 6/3/07 17:18:19
The Charlesworth Group, Wakefield +44(0)1924 369598 - Rev 7.51n/W (Jan 20 2003)

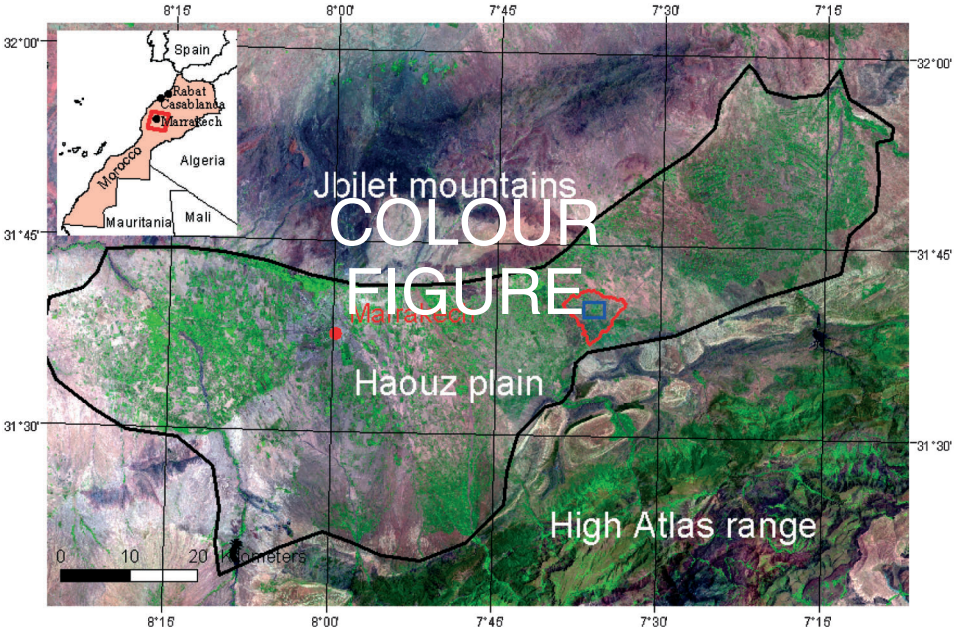

Figure 1. Overview of the study area. Colour composition dated 18 May 2003 (Thematic Mapper bands 7,4,3 respectively in R,G,B). The vegetation appears in green, corresponding mainly to irrigated crops in the Haouz plain and to natural vegetation in the High Atlas mountains. Red on the location plan indicates the frame of the full TM scenes processed. In blue on the image, the location of figure 2 (CROPSCAN); in red the area for which the cumulated ET_c is shown in figure 10.

January 2003, 11 February 2003, 27 February 2003, 31 March 2003, 16 April 2003, 18 May 2003. An image dated 8 February 2002, already corrected for reflectance, was also used as a basis for the radiometric correction of this time series.

To compute the climatic demand ET_0 required by the FAO method, we utilized the daily outputs of the ALADIN model used by the Moroccan Meteorological Services (Pailleux *et al.* 2000). This is a regional model designed for Morocco, which is constrained by daily outputs of the global model ARPEGE driven by the French National Meteorological Services. ALADIN produces every day, for a regular 16 km resolution, grid maps of the four variables used for Penmann ET_0 computation—temperature, humidity, wind speed and net radiation (all estimated at the standard height of 2 m). The outputs produced every three hours by ALADIN were averaged for each day and interpolated at the resolution of the satellite images (i.e. 30 m), using a simple bilinear interpolation. This rough interpolation was acceptable because the Haouz plain is flat and characterized by a homogeneous climate, although it would not be suitable in the High Atlas mountains, where climate is very heterogeneous and strongly linked to relief.

2.3 *Radiometric correction*

A radiometric correction was necessary to apply a deterministic identification algorithm based on analysis of the Normalized Difference Vegetation Index (NDVI) profile shape, which requires at least a relative correction of the images. These NDVI profiles will be used in a next step to estimate the phenology of the crops, in

order to estimate their water consumption, thus we also need to apply an absolute calibration to get reflectance images. Despite the increased availability of satellite images, their use is still impeded by the scarcity of good ground reflectance images, which are heavily dependent on the quality of the atmospheric parameters' input—data which is still infrequently available today—for physical modelling.

This radiometric correction was achieved in two steps. The first step was to find a set of reliable invariant objects in the raw image series, in order to get linear relation between the digital numbers (DN) of these images. Indeed, on flat areas, under reasonable assumptions of spatial homogeneity of the atmosphere, the relation between the DN of two raw images is linear (Schott *et al.* 1988). In the second step, in order to assign reflectance values to the raw images, the reflectance values of the invariant sites are linearly related to the image's DN. This simple linear correction relies on the fact that in a first approximation (for flat areas), the simplification of the radiative transfer model shows that reflectance is also a linear function of the DN of the raw image (Schott *et al.* 1988). The reflectance of the invariants was obtained using the previously computed reflectance image dated 8 February 2002. This image was available from a previous work, based on physical modelling corrections using the SMAC algorithm (Rahman and Dedieu 1994), coupled with a relative calibration (Simonneaux and François 2003).

Invariant surfaces were identified visually over the scene. The surface of each site should be at least of about 4×4 pixels to avoid positioning problems that may arise when using poorly georeferenced images. In arid zones, bare soils are widespread in landscapes and few changes occur in land cover over the course of a year. These bare soils are often good invariants (Séguis and Puech 1997). To help the identification of those sites, a pair of images was displayed on screen, manually stretched to get comparable colours. The two images were visually overlapped, making them flicker when desired, which is an efficient manner to identify candidates to serve as invariant areas. These areas were sought especially within uncultivated zones, based on the ground knowledge we have of this region. The radiometry of these areas was then displayed on the scatterplot of the same band for two dates, to check that it was on the 'no-change line' (Elvidge *et al.* 1995, Xiaojun and Lo 2000). In arid areas, this no-change line is quite visible on scatterplots for two dates and contains many pixels corresponding to bare soils that remain relatively unchanged between the two dates. This method is, in fact, less usable in temperate areas, where there are more significant changes between two dates. As precipitation is rare in the Haouz plain, and because wet soils usually dry within one or two days after an ordinary rain event, fortunately none of the images comprising the series was affected by a wet soil problem. Indeed, a wet soil occurrence would have hampered the use of this method in modifying the signature of many previously invariant objects (e.g. bare soils), making the no-change line disappear. In this way, more than 20 sites were easily identified. Such a great number may seem excessive at first glance, but it is in fact very useful to detect and eliminate outliers, i.e. pixels that may have lost their invariant property because of surface changes. Invariant corrections based on only two objects—the traditional 'dark' and 'bright' targets—may be erroneous if the observer is not absolutely sure of the quality of these points, which is often difficult to check.

The accuracy of image reflectance was assessed through a comparison with spectral measurements done during the season in wheat fields, using a CROPSCAN field spectrometer including the TM bands. This sensor is handheld, using a 3 m-

long boom leaning at 45°, which results in a patch of about 2 m^2. Because this instrument simultaneously measures both incoming solar radiation and reflected radiation—using upward and downward sensors—it is therefore less susceptible to variations of illumination during the measurements. The calibration of this spectrometer consists only of intercalibrating the upward and downward sensors in order to get correct reflectance readings, without requiring any reference panel. At the beginning of the season, the CROPSCAN measurements were checked against data collected using an ASD precision spectroradiometer. Each measurement consisted of 10 points, spaced every 10 m along a fixed transect located accurately using the GPS. The 10 points of each transect were averaged and compared with the average of the pixels corresponding to the transect line extracted from the TM image (figure 2). The wheat fields were large enough—100 m × 400 m—and homogeneous enough to minimize the potential problems of misregistration when extracting pixels related to each transect. The standard deviation (SD) of the 10 points of each transect ranged from 1 to 35%, with an average of 12%. Additional details about this measurement campaign may be found in Duchemin *et al.* (2006). 16

2.4 *Land cover characterization*

The vegetation development in the area is affected by a great heterogeneity that has consequences for the choice of a land cover classification method using remote sensing. For several crop types, especially annuals, the phenological cycles of different fields may not be synchronous, showing important shifts between fields.

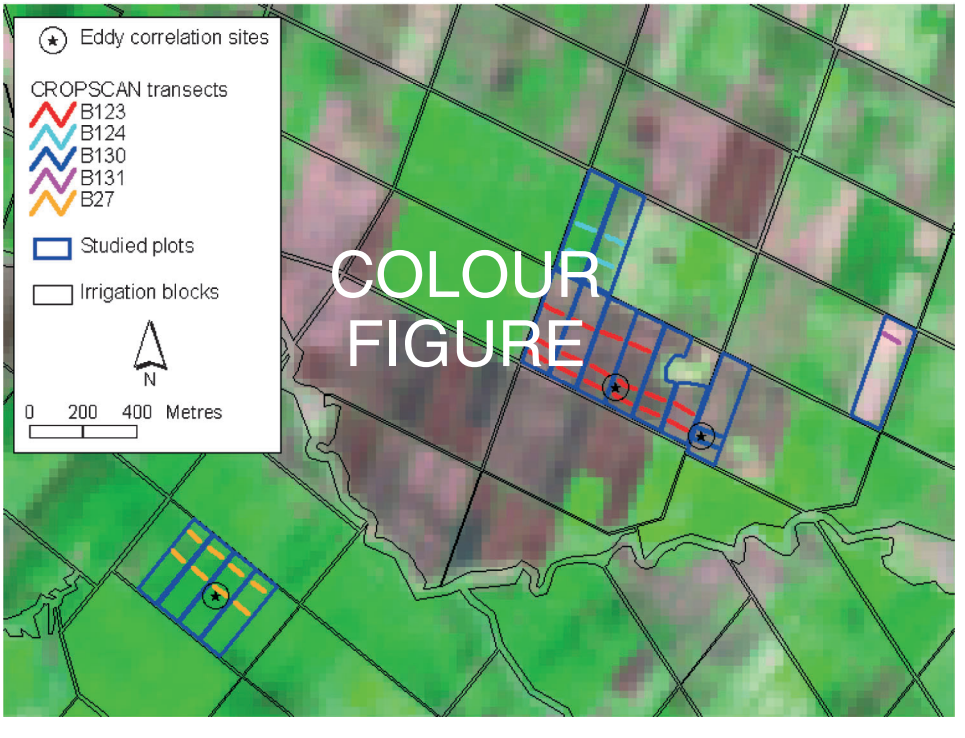

Figure 2. Location of the CROPSCAN measurements on the Thematic Mapper (TM) image dated 11 February 2003 (TM bands 7,4,3 respectively in R,G,B). The irrigated wheat displayed in various green values shows the high heterogeneity of crop development.

The phenology is indeed very dependent on agricultural practices, which may vary greatly among farmers. For financial and organizational reasons, people follow neither the same time schedule nor the same technical itineraries. For example, the sowing period for wheat ranges from November to January (Duchemin *et al.* 2006, Hadria *et al.* 2006a). One other feature of the land cover is that the cover types encountered are complex. Among tree plantations for example, there are great variations of density and age. Tree plantations also often include an understory of annual crops—wheat, grass, etc.—cultivated as forage. Thus, the land cover classes usually get very heterogeneous spectral signatures, regardless of the date considered. Moreover, there are a lot of overlapping signatures between these classes, producing spectral confusions.

For the above-mentioned reasons, we chose to focus on the analysis of the temporal behaviour of vegetation, instead of trying to use all of the spectral information available from the TM sensor through the usual classification methods such as 'maximum likelihood'. Because of the time shifts observed in agricultural practices for any particular crop, explicitly taking into account the temporal dimension of the spectral signature—for example, through the study of the vegetation index time profile—may help significantly in discriminating between classes. The identification of land cover classes based on NDVI profiles—which had previously been used mainly for low-resolution global land cover characterization (Lloyd 1990, Friedl and Brodley 1997, Chern *et al.* 2001), given that only low-resolution satellite data was readily available—has been utilized in recent years for high-resolution time series composed of fewer images by Ray and Dadhwal (2001). Using such time profiles, the identification of distinct classes may either be based on a parameterization of the NDVI profile—and on subsequent discrimination based on the estimated parameters (Liang 2001)—or it may be based on the use of simple phenological criteria, which are taken into account mainly through what are often called 'decision trees' (Lloyd 1990, Chern *et al.* 2001, Ray and Dadhwal 2001). These phenological criteria—such as the minimum, the maximum or the range of NDVI—have the advantage of bearing an ecological signification. Consequently, they are more robust than statistical criteria, which are more directly linked to the studied dataset and are therefore more difficult to generalize. The method used in our case was successfully applied during the previous season (2001/2002), using a time series of nine SPOT HRV images and a ground truth set of 120 plots that had been acquired over a smaller area (Simonneaux and François 2003). This method was adapted for the 2002/2003 season, with the assumption that we had to validate some parameters, for example the NDVI threshold used to distinguish between bare soil and vegetation. This validation was achieved based on a set of 187 field observations made during the 2002/2003 season.

2.5 *Evapotranspiration estimate*

The FAO model was chosen for the ET estimate (Allen *et al.* 1998, Allen 2000). This model is based on the assumption that any crop can be compared to a standard crop—'a well-watered grass'—from which it differs by a simple multiplicative coefficient, the 'crop coefficient', which varies over time according to the crop development.

$$ET_c = ET_0 K_c \tag{1}$$

where ET_c is the crop evapotranspiration assuming no water stress, ET_0 is the

evapotranspiration of the standard crop and K_c is the crop coefficient of the vegetation coverage studied.

The ET_0 value is computed using the Penman–Monteith equation and the following climatic parameters: air temperature, air humidity, wind speed and net radiation. The measurements fixing these parameters may be recorded on the ground in the usual way, using standard climatologic recording stations. Here we used instead the daily outputs of the ALADIN model described in §2.2, which offers a spatialization of these variables over the plain.

The main problem is to estimate the crop coefficients in space and time. For a given crop, the temporal evolution of this coefficient is modelled according to the FAO method by a trapeze curve (figure 3), with, successively, (i) a period corresponding to the seed development without significant vegetation ('initial period'); (ii) an ascending stage corresponding to the growing season ('crop development'); (iii) a stability stage corresponding to the biomass and ear development ('mid-season'); and (iv) a decreasing stage corresponding to maturity and senescence ('late season').

K_c is, in fact, a global coefficient encompassing the soil evaporation fraction of water fluxes (named K_e) and the transpiration fraction named K_{cb} for 'basal' K_c.

$$K_c = K_e + K_{cb} \tag{2}$$

Without any information about the actual crop development during the season studied, the K_c profiles used are usually the average ones found in the literature (Allen *et al.* 1998), and the beginning point of growth is arbitrarily and equally chosen for all plots, according to knowledge of the crop calendars for the region. On the other hand, if remote sensing data is available, it is possible to estimate the K_{cb}

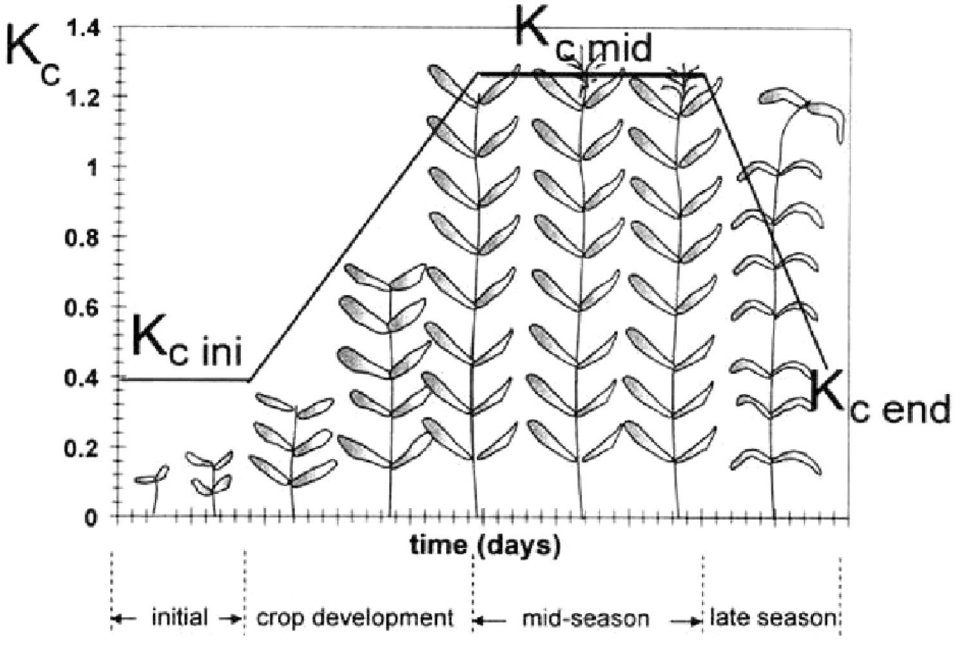

Figure 3. The *Kc* evolution of an annual crop, taken from Allen *et al.* (1998).

evolution for each pixel using image time series. The spectral information included in the images is usually closely related to vegetation phenology, especially when using vegetation indexes. Many authors have confirmed the fact that NDVI and K_{cb} can be related through a linear relation (Bausch and Neale 1987, Ray and Dadhwal 2001, Duchemin *et al.* 2006, Er-Raki *et al.* 2006). This empirical observation is easy to understand, as the K_{cb} is roughly proportional to the crop fraction cover. After the coverage reaches 100%, even if the biomass (and thus the LAI) continues to increase, the transpiration is limited by the increasing shadow and the roughness of the surface. In this case, the vegetation indexes obtained from spectral data also saturate, in correlation with the potential ET of the crop. The NDVI–K_{cb} relation was taken from the FAO guidelines (Allen *et al.* 1998):

$$K_{cb} = 1.64 \times (\mathrm{NDVI} - \mathrm{NDVI}_{min}) \quad (3)$$

with $\mathrm{NDVI}_{min} = 0.15$.

Although related to wheat, this relation will be used for all annual crops, considering that wheat is by far the main crop, and that other cereals have very similar K_{cb}. Thus, using remote sensing, it is possible to estimate NDVI for the image dates, then to interpolate a NDVI profile for each day of the vegetation season and subsequently to compute the K_{cb} using relation (3). Depending on the number of NDVI values available (i.e. the number of cloud-free dates of imagery), the interpolation method may differ. If a lot of points are available (e.g. every week), then a simple linear interpolation may be suitable. But if only three or four points are available, the linear interpolation between these sparse points would lead to an unrealistic shape of the NDVI profile. In this case, it is more reliable to assume a standard shape for the NDVI profile (i.e. a trapeze), and fit this trapeze to the points available (Duchemin *et al.* 2003). This latter method was used here to adjust an NDVI trapeze for each pixel from the points available from images. A program was coded in C++ to fit a trapeze to the available points. Seven variables were considered in adjusting the shape of the trapeze: the minimum NDVI (bare soil), the maximum NDVI (vegetation max), the sowing date and the length of the four development periods (figure 4). Theses parameters were tested iteratively using realistic value ranges and increments. The result of this fitting is—for each pixel—a specific trapeze profile matching the image points.

Unlike K_{cb}, no spatiotemporal information was available to estimate K_e. Although it may vary considerably in space and time, depending on soil water content, an arbitrary value was assumed over the growing season. However, this value was modulated for each pixel depending on its vegetation fraction cover, in order to minimize K_e when vegetation coverage is increasing. As proposed by the FAO guidelines (Allen *et al.* 1998), we used the following equation:

$$K_e = (1 - f_c) \times K_{e,\,max} \quad (4)$$

where f_c is the vegetation fraction cover: $f_c = 1.18 \times (\mathrm{NDVI}–\mathrm{NDVI}_{min})$.

$K_{e,max}$ was approximated depending on the frequency of water inputs, affecting the proportion of days with wet soil evaporating (Allen *et al.* 1998). Taking into consideration the frequency of irrigations (four to five times per season) and the rainfall events (100–250 mm rainfall during the season, very irregular), $K_{e,max}$ was fixed to a constant value of 0.3.

Finally, the K_c resulting from combining equations (3) and (4) was multiplied by the daily estimates of ET_0 to get the estimated ET_c of the crops.

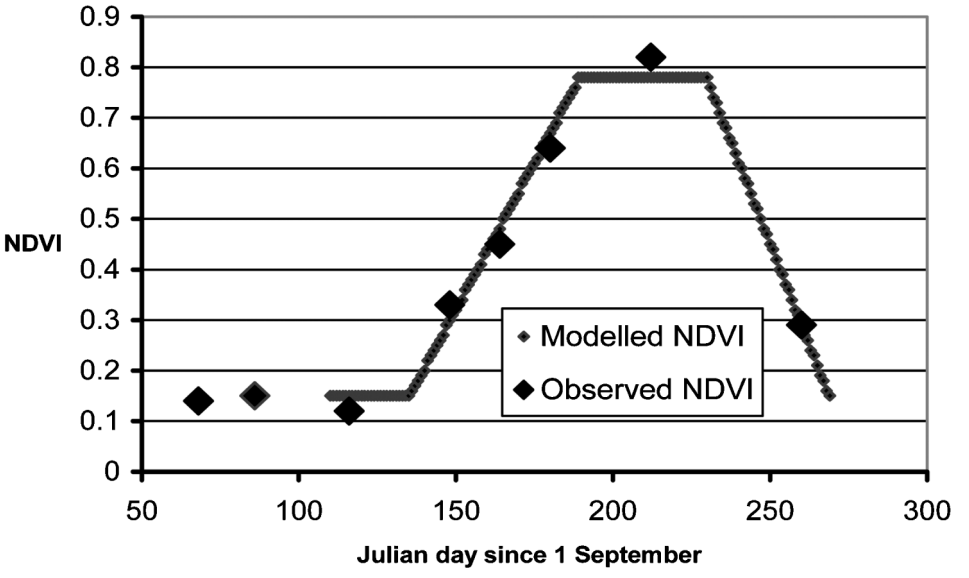

Figure 4. Modelling of the Normalized Difference Vegetation Index (NDVI) profile, example of a wheat plot with eight NDVI measurements obtained from Landsat TM images.

3. Results and discussion

3.1 *Radiometric calibration and computation of NDVI profiles*

To choose invariant areas, two images with very different vegetation development stages were selected—dated 7 November 2002 and 11 February 2003—in order to maximize the probability that invariant areas for these two dates would remain invariant for other dates. We selected 33 invariant sites in the scene, in non-vegetated areas, as flat as possible, outside the irrigated plain where there is a greater probability of their remaining stable over the course of the season. We also checked that these points were spread well over the reflectance range of the image, in order to obtain reliable regressions. Using these sites, the regression lines were computed—for each band, between pairs of images—to check for the presumed invariance of the signatures. We obtained very good determination coefficients (figure 5), usually above 0.9, showing that the areas selected are actual invariant features. Indeed, the hypothesis that all these areas might have changed such that their signatures remain proportional is highly unlikely, the invariant hypothesis being far more probable.

The 2003 images were then compared to the image dated 8 February 2002 for reflectance correction. The invariants' quality was again confirmed at this stage by the very good determination coefficients obtained. These coefficients were in the range 0.88–0.99, with an average of 0.96 (figure 6). Reflectance images were then computed using the estimated linear relations. The critical point of this correction method appears to be the source of ground reflectance information, more than the assumption of linear relation based on invariants, which appears very robust in our case.

To validate the reflectances, CROPSCAN spectral measurements were done on various dates from January to May, in 14 wheat fields in the irrigated area (Duchemin *et al.* 2006). We selected only the 69 measurements that were done within two days of an image date. The comparison with TM reflectance data shows good

International Journal of Remote Sensing res112815.3d 6/3/07 17:18:43
The Charlesworth Group, Wakefield +44(0)1924 369598 - Rev 7.51n/W (Jan 20 2003)

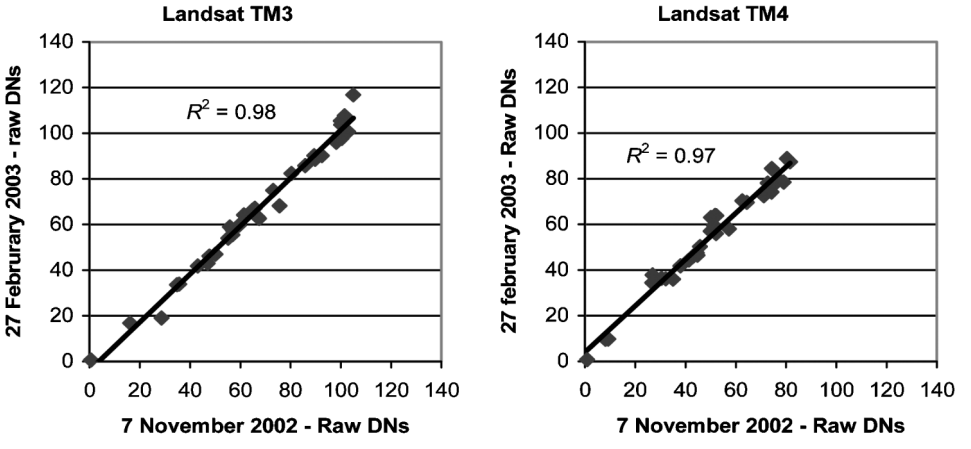

Figure 5. Comparison of raw image values for the 33 invariants. Example from images of 7 November 2002 and 27 February 2003, TM3 and TM4 bands.

agreement (figure 7) despite determination coefficients lower than those resulting from the image-to-image comparison. This is normal, since it is difficult to make field measurements comparable with image data because of the very different processes of data acquisition (Simonneaux *et al.* 2001). The main differences are the point of view and atmospheric conditions of the measurement; the time and date of the measurement; and, especially, the spatial extent of the object being measured. Image pixels are very large, even compared with transects made by handheld radiometers. Moreover, neighbouring pixels are never completely independent because of signal mixing. Thus, it is almost impossible to match the same object using field measurements, despite collecting many measurements along transects.

Nevertheless, these graphs indicate that, on the whole, the reflectance values obtained are correct. However, the relations observed show slight biases between the two data types. These biases may be due either to some problem in the radiometric correction of images—for example, that the image used as the basis for reflectance was biased—or from some bias in the spectrometer. Assuming here that

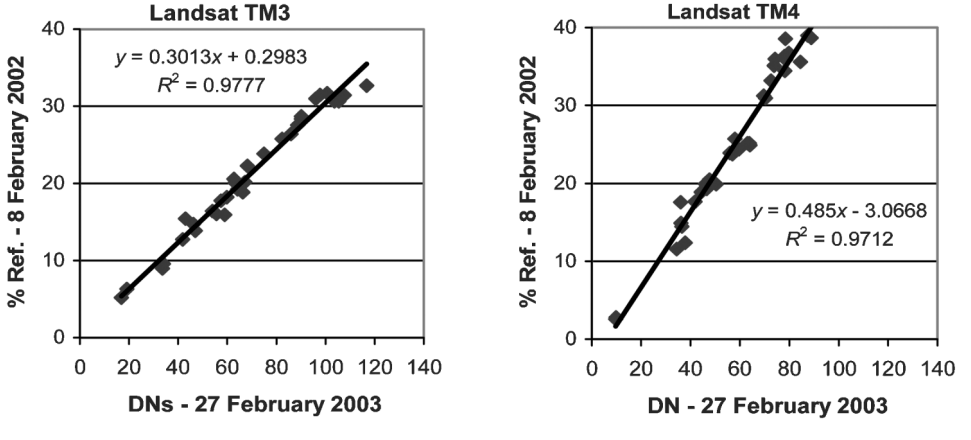

Figure 6. Relation between raw digital number (DN) values and reflectance values from 8 February 2002, for the 33 invariants. Example of 27 February 2003, TM3 and TM4 bands.

International Journal of Remote Sensing res112815.3d 6/3/07 17:18:44
The Charlesworth Group, Wakefield +44(0)1924 369598 - Rev 7.51n/W (Jan 20 2003)

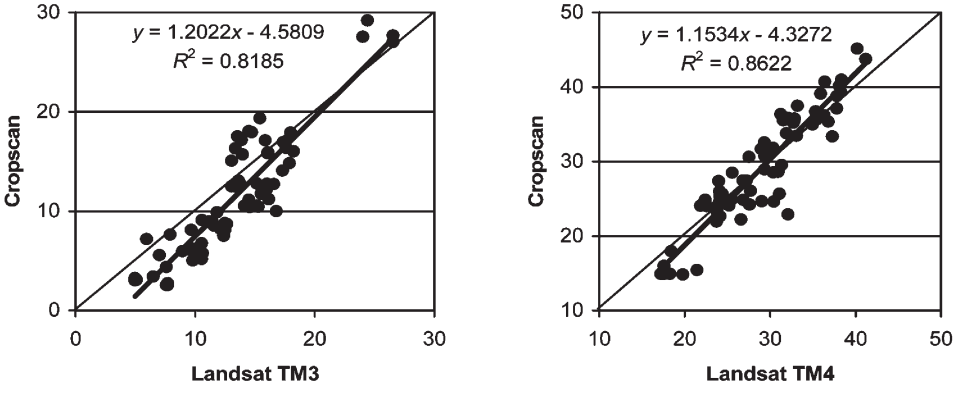

Figure 7. Relation between reflectances (%) from Thematic Mapper (TM) images and CROPSCAN ground measurements achieved between January and May 2003, for TM3 and TM4 bands.

CROPSCAN measurements were more reliable than the image reflectances, an additional correction was applied using the observed linear relations.

From the corrected image series, an NDVI profile was computed including the eight dates. Three images of the time series were partly cloudy, for dates that are very important for monitoring the crop development (27 February 2003, 31 March 2003 and 16 April 2003). Thus, instead of entirely rejecting the cloudy images, we masked the affected pixels. The clouds were small cumulus clouds, which are cold objects that are easy to identify using a simple threshold on the Landsat TM thermal band (re-sampled at 30 m). The cloud shadows were also easy to identify because they had the lowest reflectance in the near infrared (NIR) band. In order to avoid mixed pixels at the boundary of clouds and shadows, a single-pixel dilatation was applied to the generated masks. As the clouds were rarely at the same place, at least two of the three dates were usually usable for computing the NDVI profiles.

3.2 *Land cover classification*

3.2.1 Method designed using the 2001/2002 dataset. The crop identification method was designed based on a set of 120 field observations. This field data was made up of 18 thematic classes, including all the species encountered and their combinations (trees and understory). It seemed obvious that this detailed typology would not be correctly discriminated based only on the analysis of the NDVI profiles. The visual examination of the profiles showed that they might allow for a reliable discrimination of four main classes, taking into account simple phenological criteria like the minimum and maximum values of the NDVI profile and the range of NDVI over the season. These classes were bare soils, annual vegetation, trees on bare soil and trees over annual understory. The typical profiles of these four classes are shown in figure 8.

The discrimination criteria were established on the basis of three threshold values, adjusted to obtain a good discrimination of classes. These criteria were (i) the NDVI value discriminating between bare soil and vegetation (Sn=0.18); (ii) the maximum NDVI for trees on bare soil (Sa=0.40), assuming that higher NDVI depicts trees on annual understory; and (iii) the minimum NDVI range for trees on annual understory (Sr=0.2), considering that the presence of annuals would imply a

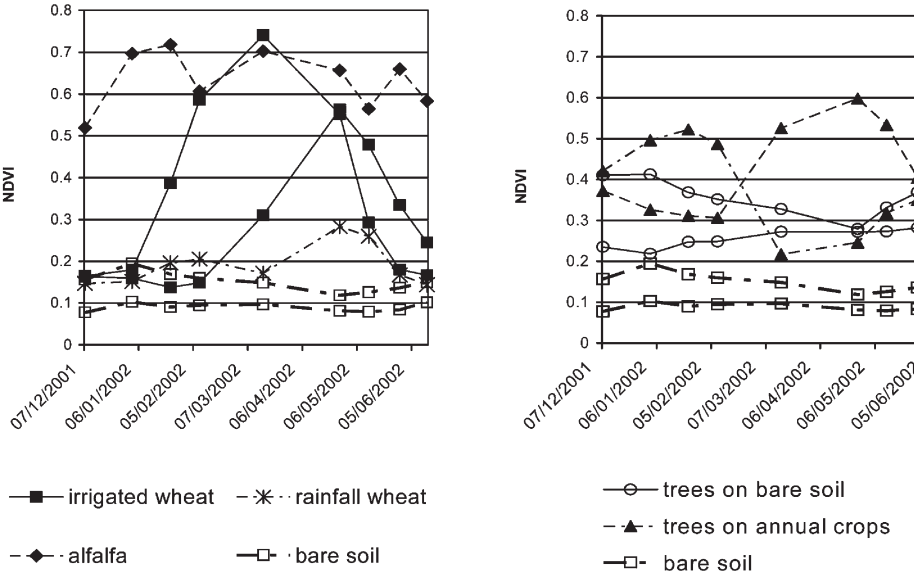

Figure 8. Normalized Difference Vegetation Index (NDVI) profiles of the main vegetation covers of the Haouz plain. Samples were visually selected on the basis of their typical shape.

minimum NDVI variation range. The resulting algorithm of classification is presented in table 1. The total number of only four classes may seem low, but it nevertheless presents valuable information for water budget assessment.

Bare soils are easy to discriminate, as they show flat and low NDVI profiles, always below a threshold *Sn*, estimated to 0.18. *Sn* may vary according to the soil properties, but no evidence was shown for that effect here, despite the presence of a large range of soil properties—texture, roughness and humidity—in the study area. These bare soils may represent either true bare soils (fallow land with almost no vegetation), or very poorly developed wheat with low NDVI.

Annual crops are defined by NDVI values rising above *Sn*, depicting significant vegetation biomass, combined with some values below *Sn*, showing non-permanent vegetation coverage (i.e. a period of bare soil). This non-vegetated period permits distinguishing them from plantations of evergreen trees, which occur frequently here. This class includes mainly cereals like wheat and barley, and some vegetables when the vegetation coverage is sufficient for NDVI rising above *Sn*.

Table 1. Criteria used for Normalized Difference Vegetation Index (NDVI) profiles classification. $Sn=0.18$, $Sa=0.4$ and $Sr=0.2$.

Conditions for NDVI values	Conditions for NDVI range	Class
All NDVI$<Sn$	No	Bare soil (SN)
Some NDVI$>Sn$ and some NDVI$<Sn$	No	Annual crops (H)
All NDVI$>Sn$	Max–Min$<Sr$ AND All NDVI$<Sa$	Trees on bare soil (ASN)
	max–min$>Sr$ or some NDVI$>Sa$	Trees + annual understory (AH)

224952

International Journal of Remote Sensing res112815.3d 6/3/07 17:18:47
The Charlesworth Group, Wakefield +44(0)1924 369598 - Rev 7.51n/W (Jan 20 2003)

Tree classes are considered as NDVI profiles always above *Sn*, considering that the majority of them are evergreen trees (olive and citrus trees). The biomass of theses trees is relatively constant over time, despite some slight variations due to growing stages and annual pruning, so their NDVI is therefore also generally constant.

Trees on bare soil are clearly identified by their having all NDVI values below a threshold $Sa=0.45$ and limited variations of NDVI (variation range $Sr<0.15$). All other tree profiles, having either high NDVI values or high NDVI ranges are considered to be *Trees on annual understory*. The distinction of these two classes is useful for water management.

The *Sn* value is critical here, because it discriminates very different classes (i.e. annuals or bare soil), which may have significant consequences when this information is later used to forecast water needs over the course of the season. But in our case, the development of the vegetation (related to K_c) is also taken into account to assess daily water requirements. Thus, the confusion between poorly developed wheat, which consumes little water, and an actual bare soil is not crucial in terms of water budgeting. The maximum value of NDVI is higher for irrigated crops, and lower for rainfall wheat. These two types of crops are usually well discriminated, but in many cases irrigated wheat that is suffering from a shortage of water will behave like rainfall wheat.

It appears that the shape of the wheat profiles is rarely a trapeze as modelled by the FAO method. However, this fact does not preclude using the method because the algorithm fitting the trapeze also fits the length of the mid-season phase and can thus fit a shorter one, as can be seen in figure 4.

Confusion may occur with some of the annual crops that show no value below *Sn* over the period of observation. This may be the case for cereals with early development compared to the first date we had available (7 November 2002). It is also the case for permanent crops like alfalfa, never showing very low NDVI values even after cutting, but which is hopefully not widespread in the study area. All these particular herbaceous crops may be confused with the tree classes, which is a more critical problem for water budgeting because these classes may show different crop coefficients.

Another problem affects young plantations, which do not show a high NDVI and are not detected on the image, even though they consume much less water than older ones. Moreover, these young plantations are usually combined with an understory of well-developed annual crops, which use most of the irrigation water, and are classified as annuals, with the related water consumption estimate.

Regarding the 2001/2002 season—for which the method was designed—the accuracy of the classification was 85% (Simonneaux and François 2003). As a basis of comparison, maximum likelihood classifications were conducted on the same dataset, using the 18 detailed classes as primary spectral classes, then combining them further to obtain the four final classes. Regardless of the number of images used—whether all of them or only a selection of dates, well-ranged over the season—the accuracy was never better than 50%. In fact, this poor result was not really surprising, considering the special features of the land cover in this area: great variability of profile shapes for some classes, and their shift on the time axis, especially for the annual covers. From the perspective of cost optimization, the NDVI profiles method was also tested using fewer images. Five images from the 2001/2002 time series, well-distributed over the season, produced results that were

equally as good as those obtained by using the full series (85%). When considering only three images—as long as they were temporally well positioned at the beginning, peak and end of the season—the accuracy was 83%.

3.2.2 Application to the 2002/2003 time series. Because annual crops change, for the 2002/2003 season a new validation set was used, based on a QuickBird very high resolution image from 24 March 2003 over a 9 km^2 subset of the area. This image was enhanced by applying a fusion of the multispectral bands (2.4 m resolution) with the panchromatic one (0.6 m resolution), giving a very sharp image on which almost all trees were visible, except for very young ones. Although the four classes were easily distinguished on this image, it was representative of a relatively small area in comparison with the extent of the Landsat images; also, the area was mainly covered with wheat. Thus, an additional field trip was carried out over the Haouz plain providing 187 observations. The confusion matrix computed using this data (table 2) gave a global accuracy of 83.7% (between 77% and 91%, depending on the class), which is close to the previous year's assessment. This positive result is not surprising, considering the simplicity of the typology and the robustness of the algorithm based on physical criteria, i.e. vegetation index analysis (the criteria were the same for both years). Unlike the method proposed by Ray and Dadhwal (2001), it is not linked to particular dates, but can be applied to any time series, assuming a reasonable distribution over the season. This is an important point from the perspective of operational application.

Because trees are long-lasting vegetation, it may be planned, in the scope of a permanent operational tool, to map such vegetation by means other than the NDVI profile shape, for example using very high resolution satellite images at metric resolution. Such a data source would produce more accurate tree mapping—reducing confusion with herbaceous perennial vegetation like alfalfa—and would improve the detection of very young trees.

3.3 *Evapotranspiration estimate*

The computation of ET_c was carried out only for annual vegetation (considered as wheat), because no accurate K_c was available for trees. The product of K_c and ET_0 was calculated for the whole vegetation cycle (i.e. from the beginning of the initial

Table 2. Confusion matrix of the 2002/2003 land cover classification (in pixels). 18

		Field observations					
		Trees on annual understory	Trees on bare soil	Annual crops	Bare soil	Total	Omission error (%)
Classification outputs	Trees on annual understory	476	73	84	13	646	26.3
	Trees on bare soil	44	392	0	12	448	17.7
	Annual crops	91	1	504	16	612	12.5
	Bare soil	6	3	5	411	425	3.3
	Total	617	469	593	452	2131	
	Omission error (%)	22.9	15	16.4	9.1		

% correctly classified=83.7, Kappa=0.78

stage to the end of the senescence stage). The cumulated ET_c was computed for the 530 000 pixels of annual crops (48 000 ha) in the Haouz plain, giving an average value of 446 mm. The distribution of the values (figure 9) shows a peak from 220 mm to 550 mm, with a mode at 415 mm. The upper tail of the histogram spreads up to 1300 mm, and probably corresponds to misclassified pixels—actually either trees or alfalfa, both of which consume much more water. The modal ET_c (415 mm) therefore seems to be more representative of the average field of annual crop. These estimates are consistent with the standard water needs as estimated by the local agency in charge of irrigation, which are 525 mm for wheat and 450 mm for barley (values issued from the application of the FAO method). Since the studied year cannot be considered as dry—with a total amount of precipitation of 300 mm for that year, compared with the climatic average of 240 mm—the difference with our estimates points to the fact that crop development is rarely optimal, owing to the aforementioned crop management problems.

For a subset of the area covered mainly with wheat (figure 10), values of cumulated ET_c vary from 200 mm to 500 mm. This very high variability is, in itself, an interesting result, which justifies the spatiotemporal approach offered by remote sensing. This high variability is not surprising; it illustrates the above-mentioned variability of farming practices—which are often not optimal, for example, with regard to the sowing or irrigation dates—more than it does the variability of intrinsic soil conditions. The higher values—around 500 mm—are those of well-conducted wheat plots experiencing almost no stress. The lower values of 200 mm correspond to wheat that is poorly developed because of water shortage or nitrogen stress that can induce large yield reduction (Hadria *et al.* 2006b). Considering the 250 mm rainfall that occurred that year from November to May, and taking into account the rainfall efficiency reducing the actual amount available for vegetation, rainfall wheat might have been able to develop and reach the lower values of ET_c observed here (around 200 mm). On the other hand, both because of problems with the availability of water and because of differences among farming practices, much of the so-called 'irrigated wheat' does not actually reach high values of ET_c. Since

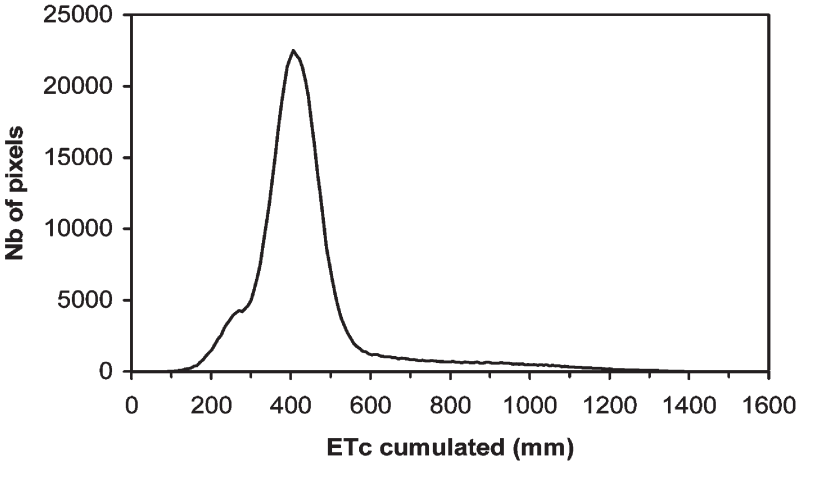

Figure 9. Histogram of cumulated ET_c for the pixels of the annual class over the whole Haouz plain.

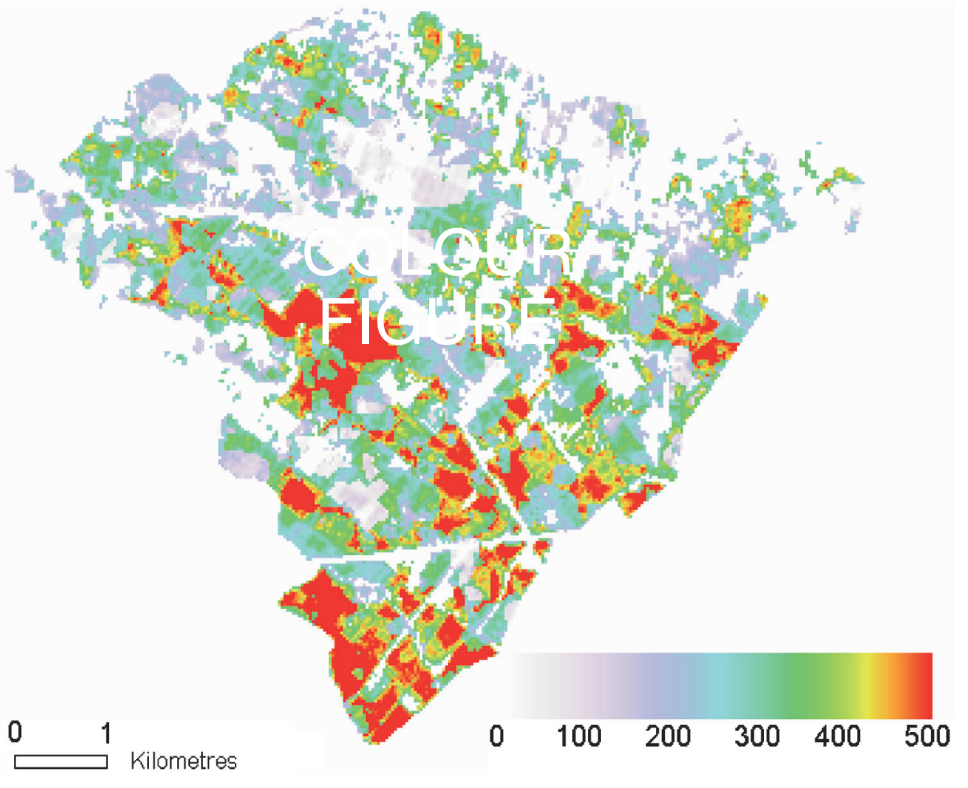

Figure 10. ET_c of annual crops cumulated over the season (mm) for an extract of the Haouz plain (see location on figure 1).

figure 10 depicts an irrigated sector, most of the wheat observed is in fact poorly developed irrigated wheat.

A first validation of these remote sensing estimates was possible thanks to ET measurements of three wheat plots, using eddy correlation systems providing measurements of the actual evapotranspiration (AET) of these plots (Duchemin *et al.* 2006, Er-Raki *et al.* 2006). The daily ET_c profiles estimated by remote sensing were extracted for the three pixels corresponding to the three eddy correlation systems (see location in figure 2). Figure 11 shows the two types of daily ET values for the three plots. The eddy correlation measurements show some gaps—especially the B123 plot—because of technical problems occurring during the experiment. On the whole, we observe concordance between the ground and remote sensing values. At the daily time step, however, there may be marked discrepancies. For the whole measurement set available, the average daily ET_c was 3.32 mm, with a daily absolute deviation of 0.89 mm (26.9%). We computed an estimate of this absolute deviation at the weekly time scale, but as there were many gaps in the time series, subsets of seven days were artificially aggregated in removing the missing days. For the 22 periods of seven days obtained, the mean daily absolute deviation was reduced to 0.61 mm (18.25%). Finally, for the whole period of measurement—about 160 days available, considering the three sites—the average daily estimate of ET_c was 3.48 mm, which means a difference of only 4.8% compared with the measurements.

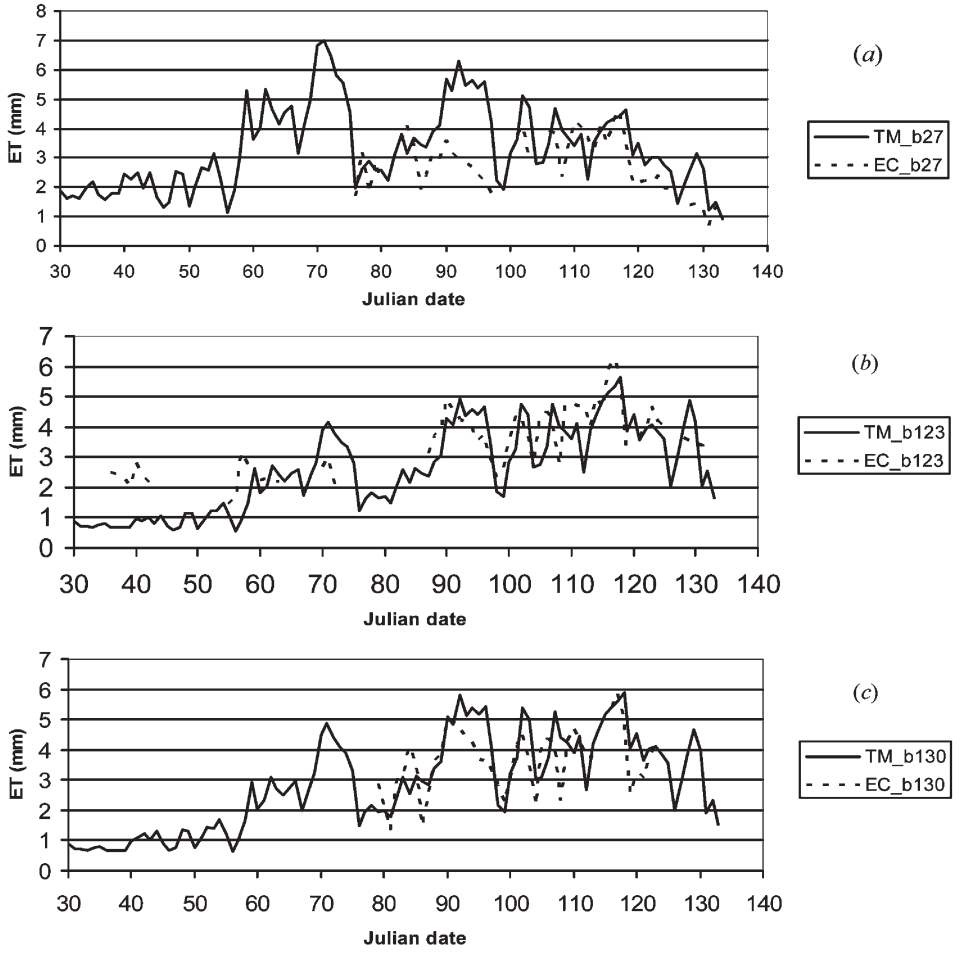

Figure 11. Comparison of ET_c estimated using FAO method and Landsat TM data (TM_ × lines) and ground measurements achieved using Eddy Correlation systems (EC_ × lines) for three plots (B27, B123, B130, see figure 2 for location). Julian days starting 1 January 2003. Note that these three plots had a very late development compared with the rest of the area.

A bigger discrepancy appears between Julian days 90 and 98 for the three plots, especially the B27 plot, where the AET decreases whereas the estimated ET_c remains at high values. This discrepancy is due to the quick rise of ET_0 during this period, coupled with a lack of irrigation, inducing stress in the vegetation. As mentioned in §2.4, the vegetation stress is not accounted for by the methodology used here. Early AET measurements were only available for plot B123, and show values much higher than the estimated ET_c for Julian days 36 to 43. This high AET corresponds to an irrigation of the plot applied on day 35, while the vegetation is still relatively undeveloped, generating a high soil evaporation that is not accounted for by our method at the daily scale, but only at the seasonal scale.

The discrepancies observed between what remote sensing offers and the AET measured on the ground mean that whatever the accuracy of NDVI and K_{cb} estimates, the ET estimated here is basically not AET. Our ET estimates are based

on NDVI—i.e. on vegetation development—but soil evaporation and vegetation stress, contributing to AET are not accurately taken into account here. The evaporation fraction of the soil, related to K_e, is considered constant, and issued empirically from the observed frequency of irrigations and rainfall events. This approximation is not satisfactory from the perspective of a spatialized monitoring at a few days' time step. The actual values of K_e may vary greatly, depending on farming practices and water availability. One remote sensing solution to overcome this problem would be the use of radar images to estimate soil moisture, but this is another field of research, currently far from being operational. The second process not being considered here is the stress of the vegetation, occurring when the soil water content is low. In the case of moderate stress, the vegetation still has the same NDVI despite a decrease in actual transpiration coefficient (Moran *et al.* 1994). To account for this stress, the FAO method introduces the stress coefficient, *Ks*, to be multiplied with K_{cb}. From a remote sensing perspective, this kind of stress may be monitored using thermal information as the reduction of transpiration makes the temperature of the plant rise, using, for example, the Water Stress Index proposed by Jackson *et al.* (1981). Thus, the ET estimated here from remote sensing is a '*pseudo*evapotranspiration'; it is both overestimated, because of potential vegetation stress, and underestimated, because of soil evaporation. In fact, the difference with AET is mainly driven by irrigation practices. For the season studied here, we see from figure 11 that the two error factors may essentially offset one another. Additionally, one should point out that the ET estimated using this method is not the potential ET resulting from ideal growing conditions. Indeed, if the stress is not considered instantaneously when it occurs, it has subsequent effects on plant growth, modifying the development of the vegetation and thereby the NDVI. The *pseudo*ET estimated here is, then, close to the actual ET most of the time, but usually below the potential ET of optimal conditions (water and nutrients). Considering the level of complexity of the modelling approach of plant stress and of soil humidity estimates using remote sensing, one simple alternative approach would be an empirical estimate of this factor adjusted to this area, as this was done for K_e.

4. Conclusion

Considering the worldwide increase of pressure on water resources, which is mainly due to its agricultural use, the accurate monitoring of agricultural water consumption over large areas is critical for planners and decision makers. In this work, we show how satellite image series may be used to estimate the evapotranspiration of crops over large areas. The availability of such satellite data is rather new and still expensive, but this should change in the next years thanks to planned or recently launched missions, such as SPOT, IRS, FORMOSAT, Venus, [20] etc.

Among the main problems to overcome, the first is the radiometric correction of satellite data to make them comparable and utilizable for physical modelling. Despite the progress made in the knowledge of atmospheric parameters, these are still often lacking or are not known accurately enough. A combined method based on physical modelling and relative correction based on invariants was proposed, which proved to be very useful for improving the results of the physical models considered alone. Regarding the relative accuracy obtained using images taken on different dates, and for a set of invariant objects, this method gave correlations between images around 0.98.

The second phase of the work was to assess land cover—a key input in estimating water consumption—using most available models, including the FAO model, which was chosen here for its compliance with and utility for remote sensing applications. The high spectral confusions between classes were overcome, giving priority to temporal analysis of the signature instead of focusing on spectral signatures. The land cover obtained is simple (annual crops, trees, annual crops + trees, bare soils) but accurate (85% well classified); it is better than the spectral classification, and relevant for the application of the FAO method. Indeed, the resulting classes match the main groups that can be distinguished in terms of water management. Problems still remain with regard to the clear identification of alfalfa, as well as in distinguishing between different types of trees. Further analysis based on more field work and using multiyear imagery would probably allow for further refinement of this first typology, permitting greater discrimination of classes—especially among trees—through the use of refined criteria.

The ultimate phase of the work was the computation of water consumption for wheat, using crop coefficients obtained from the image series. We saw that whatever the accuracy of the input variables—i.e. climatic demand (ET_0), and phenology (crop coefficients)—the main limitation is the lack of account taken of soil water content. Indeed, soil water is a key variable for water budgeting because it controls both water evaporation (when there is too much water in top soil) and plant stress (when water is lacking). The forthcoming availability of passive microwave data (SMOS mission) and the use of thermal data, associated with more complex models, should help to overcome these problems. For the time being, the simple method described here gives a first estimate of plant water consumption, assuming that top soil water evaporation is not too important, and that plant water stress is not too frequent, or at least that rough estimates of these two factors are available from empirical ground knowledge. Under this hypothesis, we show that remote sensing estimates of ET compare very satisfactorily with ground measurements.

Acknowledgment

This study was realized within the framework of the SudMed project: 'Management of hydrological and ecological resources in semi-arid areas: characterization, modelling and forecasting' (Chehbouni *et al.* 2003). This ongoing project currently involves the collaboration of CESBIO ('Center for Biosphere Study from Space', Toulouse, France) and a team of the Semlalia faculty (Cadi Ayyad University, Marrakech, Morocco), thanks to the financial support of IRD (Institute for Research in Development, France). We are grateful to the CNES (National Center for Space Studies, France) for its financial support during this work and for providing SPOT images and to the DMN (National Meteorological Directorate of Morocco) for providing us with the outputs of the ALADIN model.

References

Allen, R.G., Pereira, L.S., Raes, D. and Smith, M., 1998, *Crop evapotranspiration—Guidelines for computing crop water requirements—FAO Irrigation and drainage paper* 56 (Rome: Food and Agriculture Organization (FAO) of the United Nations).

Allen, R.G., 2000, Using the FAO-56 dual crop coefficient method over an irrigated region as part of an evapotranspiration intercomparison study. *Journal of Hydrology*, **229**, pp. 27–41.

Bastiaanssen, W.G.M., Molden, D.J. and Makin, I.W., 2000a, Remote sensing for irrigated agriculture: examples from research and possible applications. *Agricultural Water Management*, **46**, pp. 137–155.

Bastiaanssen, W.G.M., 2000b, SEBAL-based sensible and latent heat fluxes in the irrigated Gediz Basin, Turkey. *Journal of Hydrology*, **229**, pp. 87–100.

Bausch, W.C. and Neale, C.M.U., 1987, Crop coefficients derived from reflected canopy radiation: a concept. *Transactions of the ASAE*, **30**, pp. 703–709.

Calera Belmonte, A., Jochum, A.M. and Cuesta Garcia, A., 2003, Space-assisted irrigation management: towards user-friendly products. In *ICID Workshop on Remote Sensing of Crop Evapotranspiration*, 17 September, Montpellier, France.

Carlotto, M., 1998, Spectral shape classification of Landsat Thematic Mapper imagery. *Photogrammetric Engineering and Remote Sensing*, **64**, pp. 905–913.

Chehbouni, A., Escadafal, R., Dedieu, G., Errouane, S., Boulet, G., Duchemin, B., Mougenot, B., Simonneaux, V., Seghieri, J. and Timouk, F., 2003, A multi-disciplinary program for assessing the sustainability of water resources in semi-arid basin in Morocco: SUDMED. In *EGS– AGU–EUG Joint Assembly*, 6–11 April, Nice, France.

Chern, J.-S., Lee, L.-C., Wang, H.-C. and Chu, F.-H., 2001, An introduction to NSPO and ROCSATs missions. In *3rd IAA Symposium on Small Satellites for Earth Observation*, 2–6 April, Berlin, Germany.

Dedieu, G., Cabot, F., Chehbouni, A., Duchemin, B., Maisongrande, P., Boulet, G. and Pellenq, J., 2003, RHEA: a micro-satellite mission for the study and modeling of land surfaces through assimilation techniques. *EGS–AGU– EUG Joint Assembly*, 6–11 April, Nice, France.

De Fries, R.S., Hansen, M., Townshend, J.R.G. and Sohlberg, R., 1998, Global land cover classifications at 8 km spatial resolution: the use of training data derived from Landsat imagery in decision tree classifiers. *International Journal of Remote Sensing*, **19**, pp. 3141–3168.

Duchemin, B., Goubier, J. and Courrier, G., 1999, Monitoring phenological key-stages and cycle duration of temperate deciduous forest ecosystems with NOAA-AVHRR data. *Remote Sensing of Environment*, **67**, pp. 51–67.

Duchemin, B., Er-Raki, S., Gentine, P., Maisongrande, C., Coret, L., Boulet, G., Rodriguez, J.C., Simonneaux, V., Chehbouni, A., Dedieu, G. and Guemouria, N., 2003, Estimating cereal evapotranspiration using a simple model driven by satellite data. In *Proceedings of the International IEEE 2003 Geoscience and Remote Sensing Symposium (IGARSS'03)*, 21–25 July, Toulouse, France, **4**, pp. 2762–2764.

Duchemin, B., Hadria, R., Er–Raki S., Boulet, G., Maisongrande, P., Chehbouni, A., Escadafal, R., Ezzahar, J., Hoedjes, J., Karroui, H., Khabba, S., Mougenot, B., Olioso, A., Rodriguez, J–C., Simonneaux, V. and Timouk, F., 2006, Monitoring wheat phenology and irrigation in center of Morocco: on the use of relationship between evapotranspiration, crops coefficients, leaf area index and remotely sensed vegetation indices. *Agricultural Water Management*, **79**, pp. 1–27.

Er-Raki, S., Chehbouni, A., Guemouria, N., Duchemin, B., Ezzahar, J. and Hadria, R., 2006, Combining FAO-56 model and ground-based remote sensing to estimate water consumptions of wheat crops in a semi-arid region. *Agricultural Water Management* (accepted).

Elvidge, C.D., Yuan, D., Ridway, D.W. and Lunetta, R.S., 1995, Relative radiometric normalization of Landsat Multispectral Scanner (MSS) data using an automatic scattergram-controled regression. *Photogrammetric Engineering and Remote Sensing*, **66**, pp. 1255–1260.

Friedl, M.A. and Brodley, C.E., 1997, Decision tree classification of land cover from remotely sensed data. *Remote Sensing of Environment*, **61**, pp. 399–409.

224952
International Journal of Remote Sensing res112815.3d 6/3/07 17:18:58
The Charlesworth Group, Wakefield +44(0)1924 369598 - Rev 7.51n/W (Jan 20 2003)

GUTMAN, G.G., 1999, On the use of long-term global data of land reflectances and vegetation indices derived from the advanced very high resolution radiometer. *Journal of Geophysical Research*, **104**, pp. 6241–6255.

HADRIA, R., DUCHEMIN, B., LAHROUNI, A., KHABBA, S., ER-RAKI, S., DEDIEU, G. and CHEHBOUNI, A., 2006a, Monitoring of irrigated wheat in a semi-arid climate using crop modeling and remote sensing data: impact of satellite revisit time frequency. *International Journal of Remote Sensing*, (in press).

HADRIA, R., KHABBA, S., LAHROUNI, A., DUCHEMIN, B., CHEHBOUNI, A.G. and CARRIOU, J., 2006b, Calibration and validation of the STICS crop model for managing wheat irrigation in the semi-arid Marrakech/Al Haouz Plain. *Arabian Journal for Science and Engineering* (in press).

HUNSAKER, D.J., PINTER, P.J. Jr., BARNES, E.M. and KIMBALL, B.A., 2003, Estimating cotton evapotranspiration crop coefficients with a multispectral vegetation index. *Irrigation Science*, **22**, pp. 95–105.

JACKSON, R.D., REGINATO, R.J. and IDSO, S.B., 1981, Canopy temperature as a crop water stress indicator. *Water Resource Research*, **17**, pp. 1133–1138.

LIANG, S., 2001, Land-cover classification methods for multi-year AVHRR data. *International Journal of Remote Sensing*, **22**, pp. 1479–1493.

LLOYD, D., 1990, A phenological classification of terrestrial vegetation cover using shortwave vegetation index imagery. *International Journal of Remote Sensing*, **11**, pp. 2269–2279.

MAISONGRANDE, P., RUIMY, A., DEDIEU, G. and SAUGIER, B., 1995, Monitoring seasonal and interannual variations of gross primary productivity, net primary productivity and net ecosystem productivity using a diagnostic model and remotely-sensed data. *Tellus*, **47B**, pp. 178–190.

MORAN, M.S., CLARKE, T.T., INOU, Y. and VIDAL, A., 1994, Estimating crop water deficit using the relation between air-surface temperature and spectral vegetation index. *Remote Sensing of Environment*, **49**, pp. 246–263.

MOULIN, S., KERGOAT, L., VIOVY, N. and DEDIEU, G., 1997, Global scale assessment of vegetation phenology using NOAA/AVHRR satellite measurements. *Journal of Climate*, **10**, pp. 1154–1170.

PAILLEUX, J., GELEYN, J.-F. and LEGRAND, E., 2000, La prévision numérique du temps avec les modèles Arpège et Aladin: Bilan et perspectives (Numerical weather prediction with the Arpège and Aladin models; assessment and prospects). *La Météorologie*, **30**, pp. 32–60.

RAHMAN, H. and DEDIEU, G., 1994, SMAC: a simplified method for the atmospheric correction of satellite measurements in the solar spectrum. *International Journal of Remote Sensing*, **15**, pp. 123–143.

RAY, S.S. and DADHWAL, V.K., 2001, Estimation of crop evapotranspiration of irrigation command area using remote sensing and GIS. *Agricultural Water Management*, **49**, pp. 239–249.

SÉGUIS, L. and PUECH, C., 1997, Méthode de détermination des invariants radiométriques adaptée au paysage semi-aride de l'Afrique de l'Ouest. *International Journal of Remote Sensing*, **18**, pp. 255–271.

SIMONNEAUX, V. and FRANçOIS, P., 2003, Identifying main crops classes in an irrigated area using high-resolution image time series. In *Proceedings of the International IEEE Geoscience and Remote Sensing Symposium (IGARSS'03)*, 21–25 July, Toulouse, France, **1**, pp. 252–254.

SIMONNEAUX, V., BOIS, C., SCHOLTE, K. and DELAÎTRE, E., 2001, Détection d'invariants dans une série temporelle d'images satellitales en zone aride. Application à l'intercalibration des images et à la correction radiométrique d'images brutes. *International Symposium: Les régions arides surveillées depuis l'espace. De l'observation à la modélisation pour la gestion durable*, IRD/Université Cadi Ayyad, 12–15 November, Marrakech, Marocco.

224952
International Journal of Remote Sensing res112815.3d 6/3/07 17:18:58
The Charlesworth Group, Wakefield +44(0)1924 369598 - Rev 7.51n/W (Jan 20 2003)

SCHOTT, J.R., SALVAGGIO, C. and VOLCHOCK, W.J., 1988, Radiometric scene normalization using pseudoinvariant features. *Remote Sensing of Environment*, **26**, pp. 1–16.

TUCKER, C.J., 1979, Red and photographic infrared linear combinations for monitoring vegetation. *Remote Sensing of Environment*, **8**, pp. 127–150.

XIAOJUN, Y. and LO, C.P., 2000, Relative radiometric normalization performance for change detection from multi-date satellite images. *Photogrammetric Engineering and Remote Sensing*, **66**, pp. 967–980.

224952

International Journal of Remote Sensing res112815.3d 6/3/07 17:18:58
The Charlesworth Group, Wakefield +44(0)1924 369598 - Rev 7.51n/W (Jan 20 2003)